doi:10.1016/j.jmb.2006.05.015 J. Mol. Biol. (2006) 360, 409–420

JMB

Available online at www.sciencedirect.com

SCIENCE DIRECT®

ELSEVIER

A Conserved Dimer and Global Conformational Changes in the Structure of apo-PknE Ser/Thr Protein Kinase from *Mycobacterium tuberculosis*

Laurie M. Gay, Ho-Leung Ng and Tom Alber*

Department of Molecular and Cell Biology, University of California, Berkeley CA 94720-3206, USA

**Corresponding author*

The ''eukaryotic-like'' receptor Ser/Thr protein kinases (STPKs) are candidates for the sensors that mediate environmental adaptations of *Mycobacterium tuberculosis* (*Mtb*). To define the mechanisms of regulation and substrate recognition, we determined the crystal structure of the ligand-free, activated kinase domain (KD) of the *Mtb* STPK, PknE. Remarkably, the PknE KD formed a dimer similar to that first observed in the structure of the ATPγS complex of the *Mtb* paralog, PknB. This structural similarity, which occurs despite little sequence conservation between the PknB and PknE dimer interfaces, supports the idea that dimerization regulates the *Mtb* receptor STPKs. Insertion of the DFG motif into the ATP-binding site and other conformational differences compared the ATPγS:PknB complex suggest that apo-PknE is not pre-organized to bind nucleotides. This structure may represent an inactive conformation stabilized by dimerization or, alternatively, an active conformation that reveals shifts that mediate nucleotide exchange and order substrate binding.

Keywords: kinase activation; allosteric regulation; bacterial phosphosignaling; PKR; DFG motif

Introduction

Protein Ser/Thr or Tyr kinases regulate nearly all aspects of physiology in eukaryotes. Recently, bacterial genome sequences revealed the presence of ''eukaryotic-like'' Ser/Thr protein kinases (STPKs) in many pathogens.[1–3] *Mycobacterium tuberculosis* (*Mtb*), for example, encodes 11 STPKs.[4] Nine of these proteins are predicted transmembrane receptors, with an intracellular kinase domain (KD) joined through a single predicted transmembrane helix to a variable extracellular domain of six to 276 residues. Although the physiological functions of the *Mtb* STPKs are not well defined, these proteins (called PknA-L) are candidates for the regulators of diverse stages of growth, development and virulence.[5–7]

Structural and biochemical studies of *Mtb* PknB suggested that the bacterial and eukaryotic STPKs show conserved three-dimensional structures and universal mechanisms of activation and substrate recognition.[8,9] The *Mtb* KDs contain sequence motifs characteristic of the STPK family. Like many eukaryotic STPKs, the *Mtb* Pkn KDs are activated by phosphorylation of specific residues in the activation loop.[8,10] The PknB KD structure provided the first view of a bacterial STPK domain.[8,9] Despite sharing only 24% sequence identity, the ATPγS complex of the PknB KD showed a 1.4 Å backbone root-mean-square deviation (rmsd) compared to the transition-state analog complex of mouse cAMP-dependent protein kinase (PKA).[44] Conserved structural features included the closure of the N and C-terminal lobes around the nucleotide, the P loop (which binds the phosphate moieties), the catalytic loop (which contains residues required for phosphate transfer) and the DFG motif. In contrast, the αC helix and the disordered activation loop of PknB, which together form part of the binding site for protein substrates and mediate allosteric activation in response to phosphorylation, conformationally resembled inactive STPKs.[12] Thus, the PknB KD

Abbreviations used: STPK, Ser/Thr protein kinase; *Mtb*, *Mycobacterium tuberculosis*; KD, kinase domain; SAD, single wavelength anomalous diffraction.

E-mail address of the corresponding author: tom@ucxray.berkeley.edu

structure contained the key elements common to STPKs, and these elements displayed a mixture of characteristic active and inactive conformations.

Unlike most eukaryotic STPKs, the PknB KD crystallizes as a homodimer, with the contacts occurring through a surface of the N-terminal lobe on the ''back'' of the molecule relative to the active site. This contact surface, which was seen in two different crystal forms,[8,9] involves residues that are strictly conserved in PknB orthologs from diverse bacterial species.[8] This conservation, featuring the invariant Leu33′ from the adjacent monomer bound to a receptor site at the C terminus of the αC helix and dyad symmetric contacts around Tyr75, suggested strongly that the dimer interface is functional.

To explore the generality of this idea, we determined the crystal structure of a second bacterial STPK domain, that of the presumptive *Mtb* transmembrane receptor, PknE. The PknE KD shows 37% sequence identity with PknB, indicating considerable divergence of the shared fold. The function of PknE is unknown, but *in vitro* the activated KD phosphorylates Rv1747,[13] an ABC transporter of unknown specificity, and GarA, a conserved hypothetical protein.[14] The *PknE* gene is not essential for bacterial growth *in vitro* or in mice.[15,16] These results suggest a redundant function or a role in processes such as long-term infection or reactivation that have yet to be assayed.

We show here that the phosphorylated PknE KD, crystallized in the absence of nucleotide, adopts a classic STPK architecture. The absence of bound nucleotide is associated with substantial conformational differences in the apo-PknE KD compared to PknB:ATPγS. Remarkably, the PknE and PknB KDs formed similar dimers in the crystals, supporting the idea that the *Mtb* receptor STPK dimers play crucial functional roles.

Results

The PknE KD (residues 1–289) bearing an amino-terminal His_6 tag was active in autophosphorylation and transphosphorylation reactions.[13] Consistent with the results of phosphate-mapping studies,[17] mass spectrometry indicated that recombinant KD purified from *E. coli* was phosphorylated heterogeneously at five to 11 sites (Supplementary Data Figure 1). At least two phosphorylated residues occurred in the activation loop, one in the αC helix and four in the linker region between the KD and transmembrane helix. None of these phosphoryl groups was visible unambiguously in the electron density map. Analytical ultracentrifugation showed this construct is monomeric in solution (Figure 1(a)). The PknE KD was crystallized in the absence of nucleotide, and the structure of the selenomethionine-labeled protein was determined at 2.8 Å resolution using single wavelength anomalous diffraction (SAD) phasing methods (Table 1, Figure 1(b)). The refined model ($R = 0.22$, $R_{free} = 0.27$) contained two monomers in the asymmetric unit, each built as three chains composed of residues 14–160, 177–184, and 190–276.

The PknE KD (Figure 1(c) adopts the topology and bilobal structure characteristic of Hanks-type kinases.[18] No ligand was seen in the active-site cleft located between the lobes, but this space was partially occupied by the conserved DFG motif that precedes the activation loop (see below). Each of the two independent monomers showed a similar conformation (C^{α} rmsd = 0.84 Å). The two domains adopted an ''open'' conformation (Figure 1(c)) characteristic of certain ''inactive'' STPKs,[12] even though the PknE KD is phosphorylated and active in solution. No electron density was present for most of the activation loop (residues 161–176), including the phosphorylated residues in this segment.

The two independent PknE KDs in the crystals formed a dimer (Figure 1(d)). The contact surface occurred on the opposite side of the protein from the active site, holding the two catalytic clefts away from each other. The dimer interface included the C terminus of the αC helix and the adjoining αC-β4 linker segment, both of which are characteristic elements in STPKs. In many eukaryotic STPKs, the N-terminal segment of the αC helix forms part of the protein–substrate binding site, contributes to the receptor site for the phosphorylated activation loop, and positions a conserved glutamate residue (Glu64 in PknE) that forms critical contacts in the active site. Docking of the phosphorylated activation loop is thought to position the αC helix in an active conformation.[12,19] Despite phosphorylation of the PknE activation loop[17] (Supplementary Data Figure 1), this segment was disordered (rather than docking against the protein) and the αC helix was positioned up and away from the active site and the C-terminal lobe.

Strikingly, the apo-PknE KD homodimer globally resembled that observed previously in two crystal forms of nucleotide complexes of the PknB KD (Figure 2(a)).[8,9] The two catalytic domain dimers are formed through structurally analogous interfaces, but the interactions across the PknB and PknE interfaces are quite different in detail (see below). Most amino acids that form intermolecular contacts are not conserved between the PknE and PknB KDs (Figure 3). These extensive sequence changes are associated with a shift in the relative orientation of the monomers in the apo-PknE and PknB:ATPγS KD dimers (Figure 2(a)). This shift is reflected in the higher C^{α} rmsd between the two dimers (4.1 Å) compared to the PknE and PknB KD monomers (1.7 Å).

Catalytic residues and the active site

STPKs share several conserved sequence motifs and catalytic residues. Of special importance are five conserved residues (Lys45, Glu64, Asp157, Asp139 and Asn144; PknE numbering) involved in catalyzing phosphoryl transfer. In the apo-PknE KD, most of these residues are shifted significantly from the

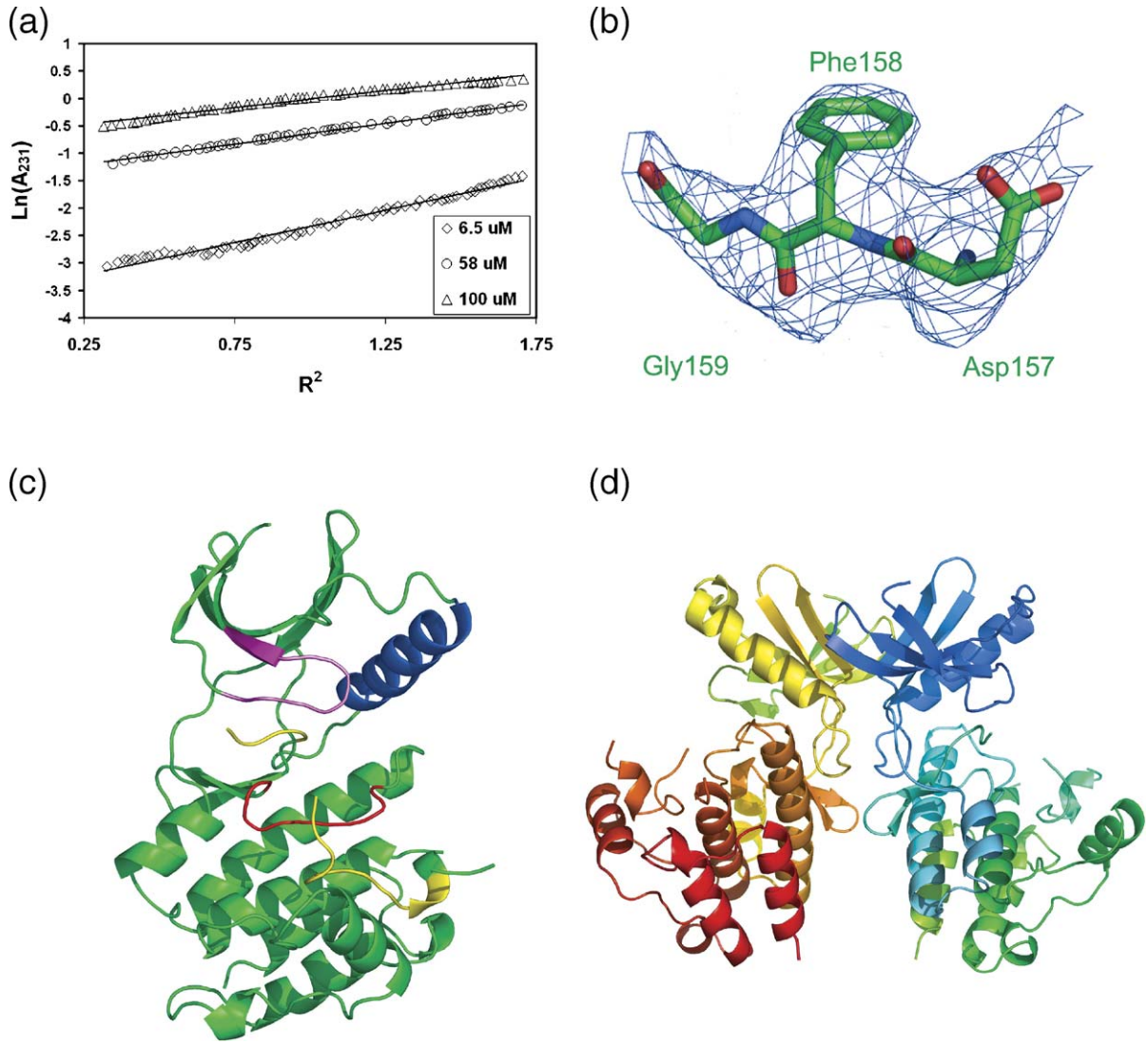

Figure 1. Structure and oligomerization of the apo-PknE kinase domain (KD). (a) Representative scans of PknE equilibrium sedimentation data (18,000 rpm) at three concentrations. Global fitting to all curves estimated a molecular mass of 32,170 Da. The calculated mass of PknE 1-289 carrying five phosphate groups is 34,040 Da. (b) SAD-phased, 2.8 Å-resolution, electron-density map (contoured at 1 σ) showing the DFG motif of monomer B. (c) PknE KD monomer showing the conserved STPK domain topology. Conserved structural and catalytic motifs include the αC helix (blue), DFG motif and activation loop (yellow), catalytic loop (red), and nucleotide-binding P loop (pink). (d) Ribbon diagram of the PknE catalytic domain dimer. The spectrum of colors from blue to green and yellow to red indicates the path of the chain from the N terminus to the C-terminus in the two monomers.

positions they occupy in an activated kinase: nucleotide complex (Figure 3(a)), as represented by the inhibitor complex of PKA.[11] Also in contrast to the structure of apo-PKA,[20] which closely resembles that of the PKA:ATP-analog complex, the active site of the PknE is not pre-organized for nucleotide binding.

Only the position of PknE Asn144, which binds divalent cations,[12] approximates that found in PKA (Figure 3(a)). In contrast, Asp157, Asp139, Glu64 and Lys45 are drastically shifted. The metal-chelating carboxylate group of Asp157 (part of the conserved DFG motif) is pointed in the opposite direction from the position seen in nucleotide-bound and apo-PKA.[11,20] PknE Glu64, a conserved residue in the αC-helix that contacts the conserved active-site lysine residue in activated STPKs, is positioned 6.8 Å from the Lys45 amino group (Figure 3(d)). The Lys45 backbone position is similar to that seen in the nucleotide complexes of PknB or PKA, but the side-chain adopts an alternate rotamer in apo-PknE. A displacement of the catalytic loop backbone orients Asp139 (homologous to PKA Asp166, which contacts the attacking substrate hydroxyl group in the PKA-ts-analog complex) out of the active site. Thus, the active site of the apo-PknE KD is not preformed for nucleotide binding, and it differs from the canonical ''active'' conformation of STPKs.

Table 1. Data collection, phasing and refinement statistics for the PknE kinase domain

Data collection and phasing	
Crystal symmetry	$P6_5$
Sample	Selenomethionine-PknE
Wavelength (Å)	0.98796
Resolution (Å)	50–2.8
Completeness (%)	100
Multiplicity	5.7 (5.8)
R_{merge} (%)	8.8 (61.5)
$<I/\sigma I>$	31.0 (2.8)
Mean figure of merit (after RESOLVE)	0.34 (0.62)
Refinement	
Resolution (Å)	34.1–2.8
Reflections	16,591
R_{cryst} (%)	21.8
R_{free} (%)	26.5
rmsd from ideal	
Bond lengths (Å)	0.010
Bond angles (deg.)	1.21
Average *B*-factor (Å^2)	74.4
Main-chain dihedral angles	
Most-favored (%)	87.3
Allowed (%)	12.7

Values in parentheses are for the highest resolution shell. $R_{merge} = \Sigma | I - <I> | / \Sigma I$, where I is intensity. F_H is the calculated heavy-atom scattering factor; E is the lack of closure error. Mean figure of merit (after density modification) $= \langle | \Sigma_\alpha P(\alpha) e^{i\alpha} / \Sigma_\alpha P(\alpha) | \rangle$, where α is the phase and $P(\alpha)$ is the phase probability distribution. $R_{cryst} = \Sigma | F_o - F_c | / \Sigma F_o$, where F_o is the observed structure-factor amplitude; and F_c is the calculated structure-factor amplitude.

Nucleotide-binding site

The apo-PknE KD structure shows substantial changes compared to the nucleotide complexes of the *Mtb* PknB KD. In addition to shifts in the locations of catalytic residues that contact the nucleotide directly (Lys45 and Asp157), the P loop and Phe158 in the DFG motif of apo-PknE occur in positions that overlap with the adenine base in the superimposed structure of the ATPγS:PknB kinase domain complex (Figure 3(b) and (c)). The P-loop residues droop toward the C lobe and limit access to the nucleotide-binding site. In this respect, the apo-PknE P-loop conformation resembles that of inactive c-Src (Figure 3(c)). Furthermore, the phenyl ring of Phe158 is buried behind this loop and occludes the binding site for the adenine ring of ATP (Figure 4(a)). Phe158 also makes contacts with several residues of the P loop, including Gly23, Arg24 and Val30.

The absence of nucleotide also releases Asp92 and Arg94 (equivalent to Glu121 of PKA)[11] from backbone interactions with adenine. The Arg94 C^α of apo-PknE is shifted 1.6 Å from the nucleotide-binding site compared to the position of the homologous residue in the PknB:ATPγS complex (Figure 4(e)). This backbone movement would likely preclude formation of hydrogen bonds between the carbonyl group of Arg94 and N1 of bound ATP. The backbone amide of Asp92 also is shifted away from the position where it could form a hydrogen bond with N6 of the superimposed adenine ring.

The DFG motif

In many activated STPK structures, the phenylalanine of the DFG motif makes contacts with residues of the αC helix that help position the helix relative to the catalytic residues and bound nucleotide.[19] As in other nucleotide-free kinases, however, the αC helix of apo-PknE is moved away from the catalytic site. The DFG motif of PknE is partially inserted into the nucleotide-binding site, with Phe158 positioned far from the αC helix (Figure 3(b)). This conformation orients the carboxylate group of Asp157 toward the back of the active site cleft, where it is unable to chelate cations or contact ATP as it would in a nucleotide complex. Phe158 is positioned in the nucleotide-binding site. Gly159 adopts ϕ, ψ dihedral angles of −179°, −35°. In the PknB:ATPγS complex, these values average −53° and 137°, reflecting a large shift that repositions the DFG motif.

Catalytic loop

The catalytic loop structure of apo-PknE, residues 137–144, also varies considerably from those of PknB:ATPγS or apo-PKA. The Arg138 and Asp139 C^α atoms are displaced at least 3.4 Å and 2.3 Å, respectively, from the positions occupied by the analogous residues in the nucleotide complexes of PknB or PKA (Figure 3(e)). The side-chain of the catalytic Asp139 adopts a different rotamer, and it is not positioned to chelate the metal ions. His137, responsible for stabilizing and orienting the DFG motif and the catalytic loop, also adopts a different rotamer and is shifted away from the active site. Asp197, a conserved residue that stabilizes the active, catalytic-loop structure in Ser/Thr and Tyr kinases through hydrogen bonds with the loop backbone, also is found in an alternate conformation, coordinating a solvent ion.

This unique conformation of the catalytic loop appears to be stabilized by a novel interaction. Hydrogen bonds are formed between the guanidinium group of Arg186 in the αEF helix, the carboxylate group of Asp139 and the backbone carbonyl group of Arg138. Arg186 immediately follows the conserved APE motif that defines the C terminus of the activation loop.

Dimer interface

The crystal structure of the apo-PknE KD establishes the presence of an equivalent dimerization interface in at least two bacterial receptor STPKs. Compared to the PknB catalytic domain, the surface area buried between PknE KD monomers is nearly 40% larger, 1404 Å^2 *versus* 1045 Å^2. The sequence positions that make intersubunit contacts in the PknB and PknE KDs are overlapping but not identical (Figure 4).

Several interactions in the PknE KD dimer interface are particularly noteworthy. Arg38′ and Arg40′ (where the prime refers to residues from the

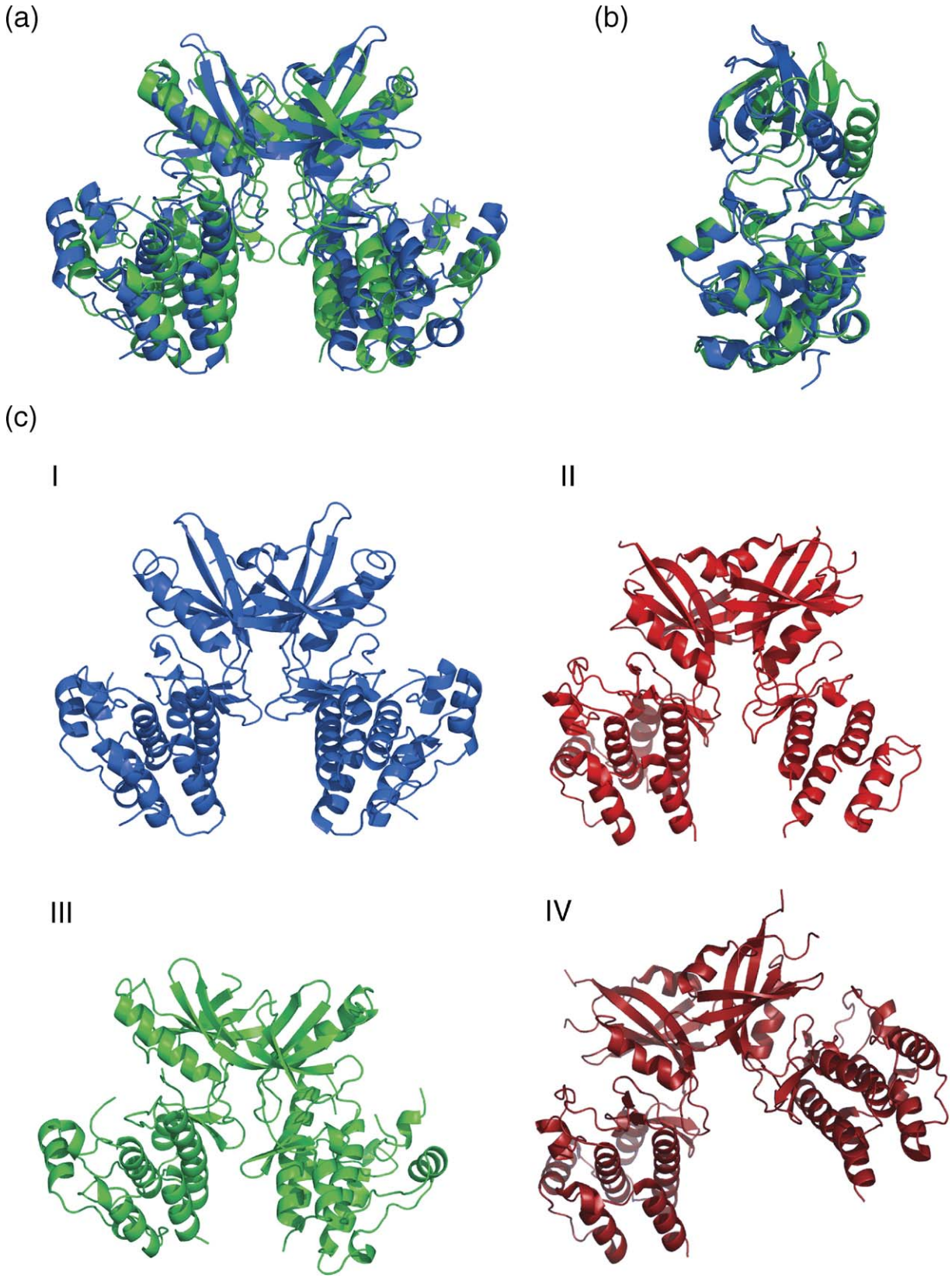

Figure 2. Similarity of PknE monomer and dimer to prokaryotic and eukaryotic STPKs. Superposition of (a) PknE KD (green) and PknB KD (blue) homodimers, aligned globally, and (b) of PknE KD and PknB KD monomers. (c) Comparison of apo-PknE KD (III, green), PknB:ATPγS (I, blue) and homodimers formed by the eukaryotic kinase, PKR, in complexes with substrates AMPPNP:eIF2α (II, red) and eIF2α alone (IV, dark red). The PKR substrates were removed to emphasize the kinase dimers. The left monomer in each structure is shown in the same orientation. The distinct positions of the other monomer in each dimer reflect differences in the dimer interfaces.

neighboring monomer) contact Phe82, which fills a pocket located near the C terminus of the αC helix. The analogous pocket in the PknB KD dimer is filled by Leu33′, which is conserved in PknB orthologs. In c-Src, Trp260 fills this site in the autoinhibited conformation (Figure 5(a)), and the Trp residue is released upon activation.[21] In the PknE KD dimer, the guanidinium group of Arg94′ also is inserted into a site formed by residues 70–79 at the C terminus of the αC helix. This interaction of Arg94′

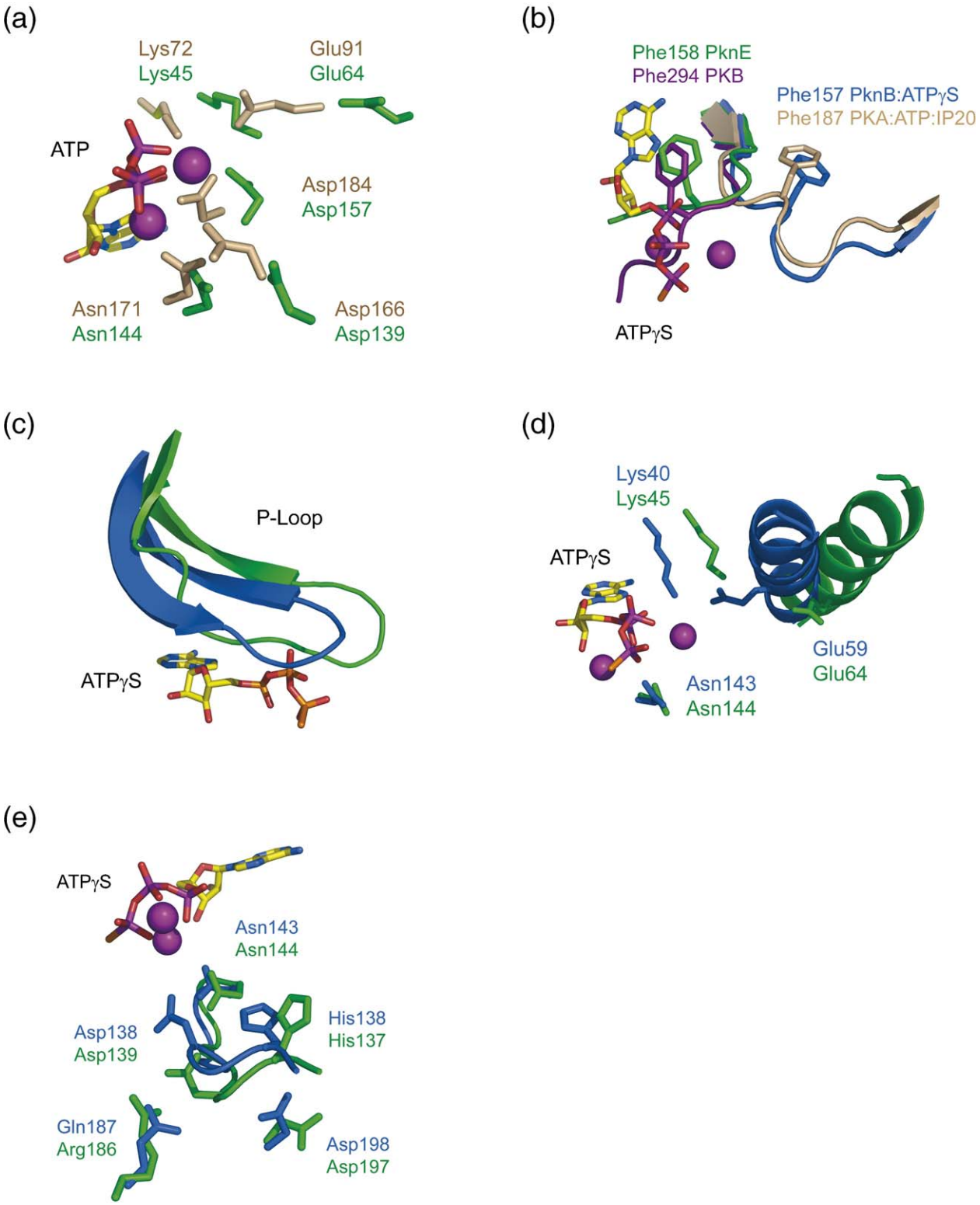

Figure 3 (*legend on opposite page*)

may influence the position of the αC helix relative to the rest of the N-lobe and the DFG motif. Residues 70–79 are further restrained by intersubunit contacts between Pro74/His75 and Phe152′/Tyr154′ in the C-terminal lobe. PknE residues Asp150, Phe152 and Tyr154 form interactions with no analogies in the PknB KD dimer. A distinctive intersubunit salt-bridge between Arg121 and Asp150′ may help define the relative rotation of the N and C-terminal lobes.

Discussion

Our results indicate that the PknE KD displays the canonical STPK fold. Although the PknE KD was monomeric in solution (Figure 1(a)), the crystal structure revealed an unexpected, structurally conserved mode of dimerization (Figures 1(d) and 2). Like the KD of PknB, apo-PknE crystallized as a homodimer with a surface opposite the active site cleft mediating intersubunit interactions. The residues in this interface are conserved in PknB orthologs and are quite distinct in PknE (Figure 4). The conservation of the PknE interface cannot be assessed, because orthologs occur only in *M. tuberculosis* and *Mycobacterium bovis*. The structural conservation of the interface in two paralogous receptor STPKs, however, supports the conclusion that dimerization is functionally important in these mycobacterial receptors. Dimerization would be promoted by the membrane localization of the KDs, as well as oligomerization of the extracellular sensor domains.

Consistent with this idea, the PknE dimer interface is structurally analogous to regulatory surfaces in certain eukaryotic STPKs. The dimer interfaces in PknE and PknB include a pocket at the C terminus of the αC helix; for example, corresponding to an allosteric autoinhibitory site in the human protein kinase c-Src (Figure 5(a)). In c-Src, Trp260 binding in this pocket is thought to maintain the KD in an inhibited state.[12,22,23] In contrast, dimerization through a structurally comparable interface (Figure 5(b)) activates PKR.[24,25] The interactions between monomers, however, are quite different in detail in PknE, PknB and PKR (Figures 2(c) and 4). The activating dimer interface of GCN2 is even more structurally distinct, even though an overlapping part of the N-lobe surface mediates intersubunit contacts.[26] In PKA,[27] additional activating contacts of the kinase C terminus may position the αC helix (Figure 5(b)). Because these bacterial and eukaryotic protein kinases are functionally diverged, the surface that mediates dimerization of PknE, PknB, PKR and GCN2 likely constitutes an important allosteric site in the STPK family.

The functions of dimerization in PknB and PknE, however, are not resolved by the crystal structures. These mycobacterial KD dimers show several features, including the tilt of the αC helix away from the active site, the absence of the conserved salt-bridge between the Lys that coordinates the α and β phosphate groups and the conserved Glu in the αC helix, and the disorder of the activation loop, often associated with inactive protein kinase structures. These features may suggest that dimerization inhibits PknB and PknE. However, the ternary substrate complex of human PKR with EIF2α and AMPPNP also shows the αC helix tilted away from the catalytic site in the active state (Figure 2(c)). Also similar to PknE and PknB, the activation loop of PKR is disordered in the kinase subunit that does not engage the eIF2α protein substrate.[24] Although both mycobacterial KDs are autophosphorylated and function catalytically, neither structure presents a fully assembled active site. Some additional assembly, perhaps promoted by substrate binding, apparently is required for the mycobacterial KDs to reach the ''active'' conformation. The role of dimerization is particularly difficult to address experimentally, because the *Mtb* KDs are heterogeneously phosphorylated,[8,10,17] and mutations in the dimer interface can alter the distribution of phosphorylation states (N. Lombana, N. Echols and T.A., unpublished results). Thus, the roles of dimerization in regulating the mycobacterial STPKs remain to be determined.

It is tempting to speculate that the structures of apo-PknE and the PknB:ATPγS complex provide distinct snapshots of the conformational transitions that occur during turnover. Both KDs were phosphorylated and active in solution.[8,13,17] Furthermore, the structures are likely to be faithful representations (rather than idiosyncratic states trapped in the crystals), because the independent monomers (two for apo-PknE and three in two crystal forms of PknB) are very similar. The interpretation of these

Figure 3. Arrangement of catalytically important motifs in apo-PknE. (a) Superposition of five important catalytic residues of the apo-PknE KD (green) and activated PKA:Mg^{2+}ATP (tan, 1ATP). The nucleotide is from the PKA complex. The kinase monomers were aligned over their C-lobes, excepting the activation loop (PknE chain B residues 100–159 and 177–276; PKA residues 127–180 and 206–262). Only Asn144/171 occurs in adopts a similar position. (b) The DFG motifs and partial activation loops from apo-PknE KD (green), the inactive conformation of PKB/Akt2 (purple), PknB:ATPγS (blue), and the activated PKA:nucleotide complex (tan). The conserved Phe158 residue is positioned in the nucleotide-binding site of the nucleotide-free kinases. The DFG motif shifts out of the active site upon nucleotide binding, and the conserved Phe interacts with the αC helix (not shown). Comparison of (c) P loop, (d) αC helix, and (e) catalytic loop in PknE (green) and PknB:ATPγS (blue). Large conformational differences can be seen. (c) The P loop in the apo-PknE KD overlaps the nucleotide in the PknB complex. (d) The PknE αC helix is shifted and rotated away form the active site, further disrupting the active-site Lys/Glu pair. (e) The distinct conformation of the apo-PknE catalytic loop is permitted by a distinct rotamer of Asp197 and stabilized by a hydrogen bond between Asp139 and Arg186.

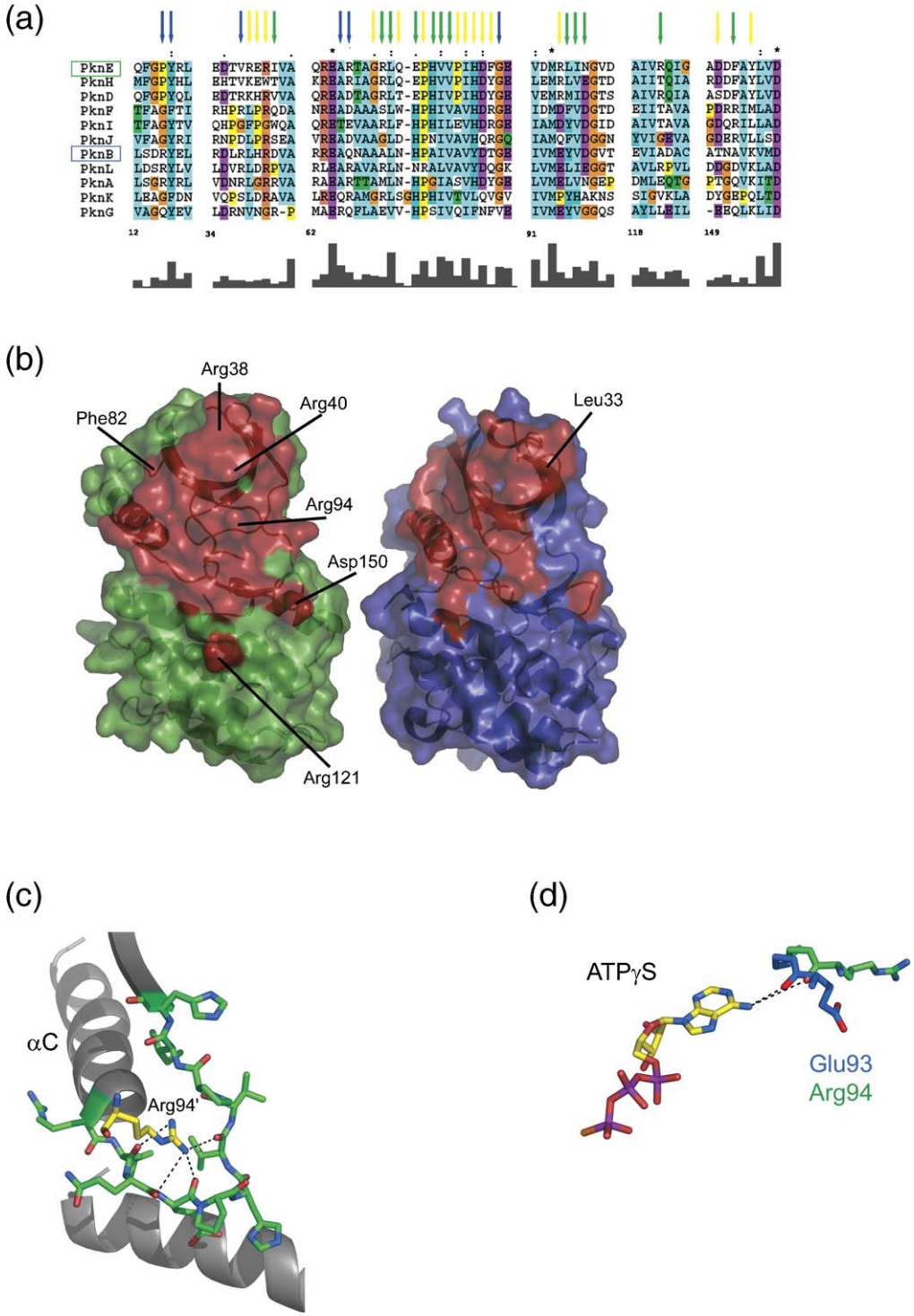

Figure 4. Dimerization interfaces of PknE and PknB. (a) Alignment of *Mtb* STPK sequences surrounding residues that make intermolecular contacts in the PknE and PknB KD homodimers. Arrows indicate the residues in the interface of PknE only (green), PknB only (blue), or both (yellow). The Clustal-X alignment was carried out using the full-length sequences of all 11 *M. tuberculosis* STPKs. The sequence numbering corresponds to PknE. Residues in the apo-PknE dimer interface include Arg38, Asp39, Arg40, Ile41, Arg66, Gly69, Arg70, Leu71, Gln72, Glu73, Pro74, His75, Val76, Pro78, Ile79, His80, Asp81, Phe82, Arg94, Leu95, Ile96, Asn97, Arg121, Asp150, Phe152 and Tyr154. Interface residues are relatively more similar in PknA, B and L; PknD, E and H; and PknF, I and J. (b) Dimer interfaces (red) shown on surface representations of the PknE (left) and PknB (right) KDs. The PknE KD dimer interface is larger than that of PknB. (c) In the PknE dimer interface, Arg 94′ (yellow) anchors the loop (green) following the αC helix of the adjacent monomer (gray, upper left). Hydrogen bonds are shown as broken lines. (d) Arg94 in the apo-PknE KD (green) is positioned in manner that is incompatible with formation of the hydrogen bond between the equivalent residue in PknB, Glu93 (blue), and the adenine ring of the bound nucleotide.

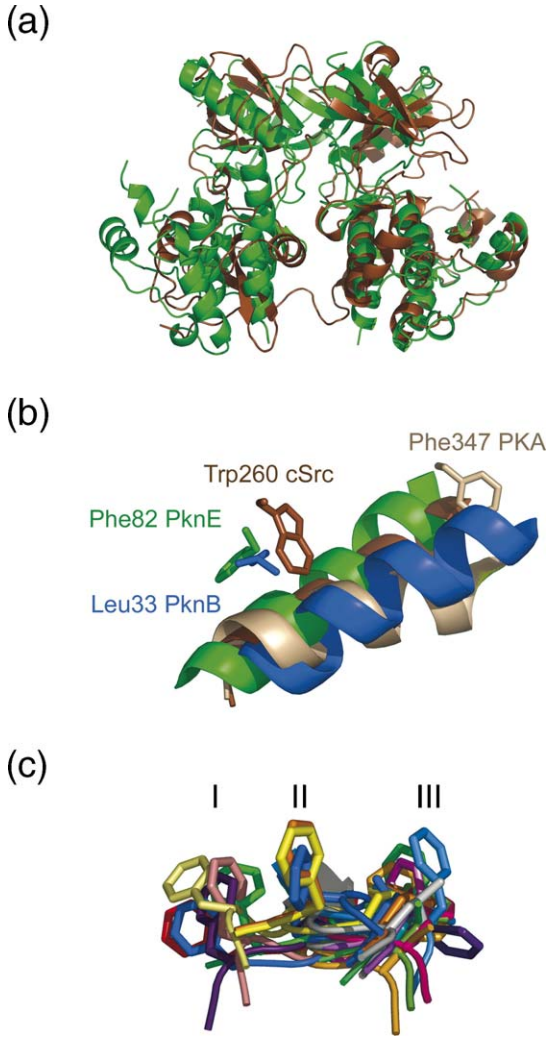

Figure 5. Comparisons of regulatory segments in prokaryotic and eukaryotic kinases. (a) Ribbon diagram showing the superposition of the right-hand monomer of the PknE KD dimer (green) and the intact autoinhibited human c-Src kinase (brown; SH2, SH3 and kinase domains) illustrating the global similarity of the allosteric interface. Both the PknE KD and c-Src are apo-enzymes. Structures were aligned over the kinase domains (PknE chain B residues 14–276 and c-Src residues 266–520). (b) Superposition of PknE (green), PknB:ATPγS (blue), c-Src (brown) and PKA (tan) showing interactions between the αC helix and regulatory hydrophobic residues. Phe82 of PknE occupies a position analogous to the inhibitory Trp260 of c-Src and Leu33′ from PknB:ATPγS. In PKA, Phe347 activates the kinase by positioning the N terminus of the αC helix. Kinase domains were aligned over the C-lobe without the activation loop. (c) The DFG motifs of inactive, unliganded kinases occupy three discrete positions in crystal structures. Apo-kinases were aligned over the helical C-lobe without the activation loop. The kinases shown are listed in Experimental Procedures. The position of the DFG motif of the activated apo-PknE KD (green, class I) resembles the extreme inward position characteristic of a subset of inactive (unphosphorylated) eukaryotic KDs.

structures is not straightforward, however, because the function of dimerization is unknown. If dimerization activates the KDs (as in PKR),[24,25] the apo-PknE KD may reveal conformational transitions involved in nucleotide exchange. In contrast, if dimerization is inhibitory, the blockade of the active site and conformational differences relative to canonical ''active'' structures may reflect the precise mechanism of inhibition.

Whether it represents an active free-enzyme conformation that changes upon nucleotide binding or a form that is inhibited stably by dimerization, the apo-PknE structure is incompatible with nucleotide binding. Of particular interest is Arg94 in the PknE dimer interface, which contacts the loop following the αC helix of the neighboring monomer (Figure 4(d)). The backbone of Arg94 is shifted out of the nucleotide-binding pocket, precluding the formation of expected hydrogen bonds with the adenine ring in the superimposed PknB:nucleotide complex (Figure 4(e)). Arg94 is structurally analogous to Glu121 of PKA, a residue in the linker region that may play a significant role in domain closure through hydrogen bond interactions with the adenine base.[28] On the basis of this analogy, the interactions between PknE Arg94 and the opposing monomer may couple the dimer interface to the nucleotide-binding site and the position of the αC helix.

Moreover, PknE Phe158 in the DFG motif is inserted into the nucleotide binding site. A small number of other apo-kinase structures contain the DFG motif in a position that does not contact either the αC helix or the catalytic loop (Figure 5(c)). Previously, the presence of the phenylalanine in the nucleotide-binding pocket was correlated with an unphosphorylated or inactive state. Alternatively, if this conformation also is adopted during the catalytic cycle in phosphorylated PknE, the DFG motif may provide a flexible, intramolecular competitor for the adenine ring to promote nucleotide release. In this sense, PknE Phe158 may be analogous to the residues of ''base-flipping'' enzymes[45] that insert into DNA to transiently stabilize the duplex structure while the substrate base is unstacked. In either case, the shifts of Phe158 into and out of the active site can signal the nucleotide status of the enzyme.

The observation of a structurally conserved PknE KD dimer limits models for the mechanism of PknE activation. The PknE KD is connected through a single predicted transmembrane helix to a 207 residue extracellular domain. The fold of the PknE extracellular sensor domain was predicted by CDART[46] (E-value $= 4 \times 10^{-19}$) and PHYRE† (E-value $= 3.7 \times 10^{-12}$) to resemble the disulfide bond catalyst, DsbG. The PknE sensor domain sequence contains the signature CXXC motif that characterizes the active sites of the thioredoxin superfamily members.[29,30] The XX residues influence redox potential, and the CPPC motif found in PknE has been shown to reduce the redox potential and catalytic activity of DsbA.[31,32]

† http://www.sbg.bio.ic.ac.uk/~phyre/

Moreover, the residues surrounding the active site, such as the Thr-Pro in the ''*cis*-Pro loop'', are more characteristic of disulfide-bond isomerases than reductases.[33]

The strong prediction that the PknE sensor domain contains an intramolecular disulfide bond suggests that this receptor STPK may respond to the reducing power of the environment or of particular extracellular proteins. *Mtb* grows in environments, including aerobic conditions outside the host, a more reducing environment inside the host cell, or in oxygen-depleted regions of granulomas,[5] that differ significantly in reducing power. The dimerization of the PknE KD through a structurally conserved allosteric interface implies that the redox signal may be coupled to kinase activity through receptor-kinase oligomerization. The structure of the PknE KD lays the groundwork to test this model *in vitro* and *in vivo*.

Experimental Procedures

Cloning, expression, and purification

N-terminally His_6-tagged PknE 1-289 was expressed from a pET28b vector (Novagen) constructed using sticky-end PCR.[34] PCR products were generated from *M. tuberculosis* H37Rv genomic DNA obtained from the TB Materials and Vaccine Testing Contract at Colorado State University. The construct was confirmed by DNA sequencing.

The expression vector was transformed into BL21 Codon Plus (DE3) cells (Stratagene) for expression of both native and selenomethionine-labeled protein. Native protein was expressed by auto-induction,[35] and purified by Ni^{2+}-agarose affinity chromatography. Selenomethionine-labeled protein was expressed as described,[36] and purified by Ni^{2+}-affinity, size-exclusion and ion-exchange chromatography. The purified PknE KD was dialyzed into 25 mM Hepes (pH 7.5), 50 mM NaCl, 0.5 mM Tris(2-carboxyethyl)-phosphine (TCEP).

Mass Spectrometry

N-terminally His_6-tagged PknE 1-289 was dialyzed into 100 mM Tris–HCl (pH 8), and digested fully with trypsin (Sigma) at a protease-to-kinase ratio of 1:100 (w/w). Phosphopeptides were isolated using Fe^{III}-chelated magnetic beads and eluted with 0.1% (w/v) ammonium acetate, pH 10. The eluate was lyophilized, dissolved in 10 μl of 5% (v/v) formic acid, centrifuged, and 5 μl was applied to a 10 cm × 100 μm Polaris C18 reverse-phase column set up as a nanospray source for the mass spectrometer. The column was eluted with a linear gradient from 0 to 45% buffer B in 110 min, where buffers A and B were 5% (v/v) acetonitrile, 0.02% (v/v) heptafluorobutyric acid and 80% acetonitrile/0.02% heptafluorobutyric acid, respectively. Data were collected using a ThermoFinnigan LCQ DecaXP Plus ion + trap mass spectrometer. Fragmentation spectra were collected for the three most abundant ions in the mass spectrum with dynamic exclusion enabled. Sequences were assigned using the program Sequest, searching for phosphorylation on STY as +79.98 and on ST as −18.0. Putative phosphopeptide spectra were inspected individually for the presence of a neutral-loss peak for phosphate.

Purified PknE 1-289 carrying a C-terminal His_6 tag was analyzed on a Bruker/Agilent Esquire-LC ion-trap mass spectrometer to determine the KD phosphorylation state (Supplemental Data Figure 1). Spectra were deconvoluted using the Protein Reconstruct algorithm from BioAnalyst (Applied Biosystems).

Analytical ultracentrifugation

Equilibrium sedimentation was performed using a Beckman Coulter XL-1 Optima analytical ultracentrifuge equipped with an An60Ti rotor. His_6-tagged PknE 1-289 in 25 mM Hepes (pH 7.9), 50 mM NaCl, 0.1 mM Tris(2-carboxyethyl)-phosphine, was equilibrated at 18,000 rpm and 24,000 rpm at 20 °C, and scans were collected at 231 nm. Measurements were made in triplicate on protein samples with concentrations of 6.5 μM, 58 μM, and 100 μM. Protein concentrations were determined by UV spectrometry at 280 nm using a molar extinction coefficient of 14,440 M^{-1} cm^{-1}. Data were analyzed using Ultrascan v. 7.2.[37,47] The data conformed well (34.3%) to the one-component, ideal model and conformed poorly to the monomer-dimer model (calculated $K_D = 2$ mM).

Crystallization and data collection

Crystals of apo-PknE KD were obtained at 18 °C by vapor diffusion against 0.1 M Hepes (pH 7.0) 12% (w/v) PEG-8000, 0.2 M NaBr using hanging drops. PknE KD (2 μl at 5 mg/ml with 1 mM $MnCl_2$) was combined with 2 μl of the well solution. Crystals appeared after four to seven days. Crystals were transferred to cryoprotectant solution containing 25% (v/v) ethylene glycol in the mother liquor and flash-frozen in liquid nitrogen. Native crystals diffracted to 3 Å resolution. Selenomethionine-substituted crystals were obtained by microbatch crystallization in the same condition using 1:9 (v/v) mixture of silicon/paraffin oil to cover the drops. Optimal crystallization occurred after approximately 12–20 h at room temperature, followed by incubation at 18 °C. These crystals, also frozen in mother liquor containing 25% ethylene glycol, diffracted to 2.8 Å resolution. Diffraction data were collected at beamline 8.3.1 at the Advanced Light Source, Lawrence Berkeley National Laboratory. Data were integrated and scaled using the program HKL2000.[38]

Structure determination and refinement

Of the 22 selenomethionine sites in the PknE KD dimer, 18 were located using the programs SOLVE/RESOLVE,[39,40] employing SAD methods. The structure of PknB (1MRU) was docked manually into the initial electron density map, and rigid body refinement was performed using REFMAC5.[41,42] The model was rebuilt using the program O.[42] Further restrained refinement was carried out using REFMAC5. A single overall *B*-value was used in the early stages of the refinement. Composite omit maps generated using CNS were used to guide rebuilding.[43] TLS parameters defining each of the four major lobes individually were used in late stages of refinement. The final model includes residues 14–159, 177–184, and 190–276, and restrained individual *B*-values

for the atoms. Residues 22–30 and 46–61 in the N-terminal lobe showed C^{α} *B*-values above 85 $Å^2$ in both subunits. Other key residues (94, 137–141, 157–160 and 197) had C^{α} *B*-values in the 70–80 $Å^2$ range, typical of structures at this resolution. The C-helix (residues 55–70) showed a pattern of C^{α} *B*-values decreasing from the N terminus to the C terminus in the dimer interface.

Coordinates

For structural comparisons, we used the following structures: PknB (1MRU), PKA inhibitor complex (1ATP), apo PKA (1J3H), apo PKB/Akt2 (1MRY), PKR-substrate complexes (2A19 and 2A1A) and cSrc (1FMK).

The following apo-STPK structures were used to compare DFG motifs: PKA (1J3H), PKB (1MRY), ERK2 (1ERK), GSK-3β (1H8F), Jnk1 (1UKH), P38 (1P38; 1WFC), c-KIT (1T45), c-Src (1FMK), FGFR1K (1FGK), Flt3 (1RJB), IGF1RK (1M7N), Irk (1IRK), Tie2 (1FVR), Musk (1LUF), PAK1 (1F3M), GrK2 (1OMW), Sky1P (1Q8Z), Syk (1XBA), Gcn2 (1ZYC), Igf-1R (1P4O), CDK2 (1PW2), CK2 (1JAM), DAP (1JKS), ITK/TSK (1SNX).

Databank Accession Number

The coordinates and structure factors of the PknE KD have been deposited in the protein databank with accession number 2H34.

Acknowledgements

We thank Tracy Young and Poh Kheng Teng for assistance with protein production; David King and Lori Kohlstaedt for mass spectrometry; T. Noelle Lombana for assistance with analytical ultracentrifugation; James Holton, Jane Tanamachi and George Meigs for assistance with X-ray data collection; and Nat Echols and Emmanuel Skordalakes for helpful suggestions during model building and refinement. We are indebted to T. Terwilliger and the TB Structural Genomics Consortium for support. This work was supported by a grant from the NIH and a Ruth L. Kirschstein National Research Service Award. Beamline 8.3.1 at the Advanced Light Source was funded by the NSF, the University of California and Henry Wheeler.

Supplementary Data

Supplementary data associated with this article can be found, in the online version, at doi:10.1016/j.jmb.2006.05.015

References

1. Zhang, C. C. (1996). Bacterial signalling involving eukaryotic-type protein kinases. *Mol. Microbiol.* **20**, 9–15.
2. Shi, L., Potts, M. & Kennelly, P. J. (1998). The serine, threonine, and/or tyrosine-specific protein kinases and protein phosphatases of prokaryotic organisms: a family portrait. *FEMS Microbiol. Rev.* **22**, 229–253.
3. Kennelly, P. J. (2002). Protein kinases and protein phosphatases in prokaryotes: a genomic perspective. *FEMS Microbiol. Letters*, **206**, 1–8.
4. Cole, S. T., Brosch, R., Parkhill, J., Garnier, T., Churcher, C., Harris, D. *et al.* (1998). Deciphering the biology of *Mycobacterium tuberculosis* from the complete genome sequence. *Nature*, **393**, 537–544.
5. Russell, D. G. (2001). *Mycobacterium tuberculosis*: here today, and here tomorrow. *Nature Rev. Mol. Cell Biol.* **2**, 569–577.
6. Greenstein, R. J. (2003). Is Crohn's disease caused by a mycobacterium? Comparisons with leprosy, tuberculosis, and Johne's disease. *Lancet Infect. Dis.* **3**, 507–514.
7. Av-Gay, Y. & Everett, M. (2000). The eukaryotic-like Ser/Thr proteins of Mycobacterium tuberculosis. *Trends Microbiol.* **8**, 238–244.
8. Young, T. A., Delagoutte, B., Endrizzi, J. A., Falick, A. M. & Alber, T. (2003). Structure of Mycobacterium tuberculosis PknB supports a universal activation mechanism for Ser/Thr protein kinases. *Nature Struct. Biol.* **10**, 168–174.
9. Ortiz-Lombardia, M., Pompeo, F., Boitel, B. & Alzari, P. M. (2003). Crystal structure of the catalytic domain of the PknB serine/threonine kinase from *Mycobacterium tuberculosis*. *J. Biol. Chem.* **278**, 13094–13100.
10. Boitel, B., Ortiz-Lombardia, M., Duran, R., Pompeo, F., Cole, S. T., Cervenansky, C. & Alzari, P. M. (2003). PknB kinase activity is regulated by phosphorylation in two Thr residues and dephosphorylation by PstP, the cognate phospho-Ser/Thr phosphatase, in *Mycobacterium tuberculosis*. *Mol. Microbiol.* **49**, 1493–1508.
11. Zheng, J., Trafny, E. A., Knighton, D. R., Xuong, N. H., Taylor, S. S., Ten Eyck, L. F. & Sowadski, J. M. (1993). 2.2 Å refined crystal structure of the catalytic subunit of cAMP-dependent protein kinase complexed with MnATP and a peptide inhibitor. *Acta Crystallog. sect. D* **49**, 362–365.
12. Huse, M. & Kuriyan, J. (2002). The conformational plasticity of protein kinases. *Cell*, **109**, 275–282.
13. Grundner, C., Gay, L. M. & Alber, T. (2005). *Mycobacterium tuberculosis* serine/threonine kinases PknB, PknD, PknE, and PknF phosphorylate multiple FHA domains. *Protein Sci.* **14**, 1918–1921.
14. Villarino, A., Duran, R., Wehenkel, A., Fernandez, P., England, P., Brodin, P. *et al.* (2005). Proteomic identification of M. tuberculosis protein kinase substrates: PknB recruits GarA, a FHA domain-containing protein, through activation loop-mediated interactions. *J. Mol. Biol.* **350**, 953–963.
15. Sassetti, C. M. & Rubin, E. J. (2003). Genetic requirements for mycobacterial survival during infection. *Proc. Natl Acad. Sci. USA*, **100**, 12989–12994.
16. Sassetti, C. M., Boyd, D. H. & Rubin, E. J. (2003). Genes required for mycobacterial growth defined by high density mutagenesis. *Mol. Microbiol.* **48**, 77–84.
17. Duran, R., Villarino, A., Bellinzoni, M., Wehenkel, A., Fernandez, P., Boitel, B. *et al.* (2005). Conserved autophosphorylation pattern in activation loops and juxtamembrane regions of *Mycobacterium tuberculosis* Ser/Thr protein kinases. *Biochem. Biophys. Res. Commun.* **333**, 858–867.

18. Hanks, S. K. & Hunter, T. (1995). The eukaryotic protein kinase superfamily: kinase (catalytic) domain structure and classification. *FASEB J.* **9**, 576–596.
19. Nolen, B., Taylor, S. & Ghosti, G. (2004). Regulation of protein kinases: controlling activity through activation segment conformation. *Mol. Cell* **15**, 661–675.
20. Akamine, P., Madhusudan, J. W., Nguyen-Huu, X., Ten Eyck, L. F. & Taylor, S. S. (2003). Dynamic features of cAMP-dependent protein kinase revealed by apoenzyme crystal structure. *J. Mol. Biol.* **327**, 159–171.
21. Boggon, T. J. & Eck, M. J. (2004). Structure and regulation of Src family kinases. *Oncogene*, **23**, 7918–7927.
22. Xu, W., Doshi, A., Lei, M., Eck, M. J. & Harrison, S. C. (1999). Crystal structures of c-Src reveal features of its autoinhibitory mechanism. *Mol. Cell,* **3**, 629–638.
23. Young, M. A., Gonfloni, S., Superti-Furga, G., Roux, B. & Kuriyan, J. (2001). Dynamic coupling between the SH2 and SH3 domains of c-Src and Hck underlies their inactivation by C-terminal tyrosine phosphorylation. *Cell*, **105**, 115–126.
24. Dar, A. C., Dever, T. E. & Sicheri, F. (2005). Higher-order substrate recognition of eIF2alpha by the RNA-dependent protein kinase PKR. *Cell*, **122**, 887–900.
25. Dey, M., Cao, C., Dar, A. C., Tamura, T., Ozato, K., Sicheri, F. & Dever, T. E. (2005). Mechanistic link between PKR dimerization, autophosphorylation, and eIF2alpha substrate recognition. *Cell*, **122**, 901–913.
26. Padyana, A. K., Qiu, H., Roll-Mecak, A., Hinnebusch, A. G. & Burley, S. K. (2005). Structural basis for autoinhibition and mutational activation of eukaryotic initiation factor 2alpha protein kinase GCN2. *J. Biol. Chem.* **280**, 29289–29299.
27. Taylor, S. S., Yang, J., Wu, J., Haste, N. M., Radzio-Andzelm, E. & Anand, G. (2004). PKA: a portrait of protein kinase dynamics. *Biochim. Biophys. Actam* **1697**, 259–269.
28. Hayward, S. (2004). Identification of specific interactions that drive ligand-induced closure in five enzymes with classic domain movements. *J. Mol. Biol.* **339**, 1001–1021.
29. Raina, S. & Missiakas, D. (1997). Making and breaking disulfide bonds. *Annu. Rev. Microbiol.* **51**, 179–202.
30. Collet, J. F. & Bardwell, J. C. (2002). Oxidative protein folding in bacteria. *Mol. Microbiol.* **44**, 1–8.
31. Bessette, P. H., Qiu, J., Bardwell, J. C., Swartz, J. R. & Georgiou, G. (2001). Effect of sequences of the active-site dipeptides of DsbA and DsbC on in vivo folding of multidisulfide proteins in *Escherichia coli*. *J. Bacteriol.* **183**, 980–988.
32. Chivers, P. T., Prehoda, K. E. & Raines, R. T. (1997). The CXXC motif: a rheostat in the active site. *Biochemistry*, **36**, 4061–4066.
33. Heras, B., Edeling, M. A., Schirra, H. J., Raina, S. & Martin, J. L. (2004). Crystal structures of the DsbG disulfide isomerase reveal an unstable disulfide. *Proc. Natl Acad. Sci. USA,* **101**, 8876–8881.
34. Zeng, G. (1998). Sticky-end PCR: new method for subcloning. *BioTechniques*, **25**, 206–208.
35. Studier, F. W. (2005). Protein production by auto-induction in high density shaking cultures. *Protein Exp.r Purif.* **41**, 207–234.
36. Van Duyne, G. D., Standaert, R. F., Karplus, P. A., Schreiber, S. L. & Clardy, J. (1993). Atomic structures of the human immunophilin FKBP-12 complexes with FK506 and rapamycin. *J. Mol. Biol.* **229**, 105–124.
37. Johnson, M. L., Correia, J. J., Yphantis, D. A. & Halvorson, H. R. (1981). Analysis of data from the analytical ultracentrifuge by nonlinear least-squares techniques. *Biophys. J.* **36**, 575–588.
38. Otwinowski, Z. & Minor, W. (1997). Processing of X-ray diffraction data collected in oscillation mode. *Methods Enzymol.* **276**, 307–326.
39. Terwilliger, T. C. (2000). Maximum-likelihood density modification. *Acta Crystallog. sect. D* **56**, 965–972.
40. Terwilliger, T. C. & Berendzen, J. (1999). Automated MAD and MIR structure solution. *Acta Crystallog. sect. D,* **55**, 849–861.
41. Skubak, P., Murshudov, G. N. & Pannu, N. S. (2004). Direct incorporation of experimental phase information in model refinement. *Acta Crystallog. sect. D,* **60**, 2196–2201.
42. Jones, T. A., Zou, J. Y., Cowan, S. W. & Kjeldgaard, M. (1991). Improved methods for building protein models in electron density maps and the location of errors in these models. *Acta Crystallog. sect. A,* **47**, 110–119.
43. Brunger, A. T., Adams, P. D., Clore, G. M., DeLano, W. L., Gros, P., Grosse-Kunstleve, R. W. *et al.* (1998). Crystallography and NMR system: a new software suite for macromolecular structure determination. *Acta Crystallog. sect. D,* **54**, 905–921.
44. Madhusudan, Akamine, P., Xuong, N.-H. & Taylor, S. S. (2002). Crystal structure of a transition state mimic of the catalytic subunit of cAMP-dependent protein kinase. *Nature Struct. Biol.* **9**, 273–277.
45. Roberts, R. J. & Cheng, X. (1998). Base flipping. *Annu. Rev. Biochem.* **67**, 181–198.
46. Marchler-Bauer, A. & Bryant, S. H. (2004). CD-Search: protein domain annotations on the fly. *Nucleic Acids Res.* **32**, W327–W331.
47. McRorie, D. & Voelker, P. (1993). *Self-Associating Systems in the Analytical Ultracentrifuge*. Fullerton, CA: Beckman Instruments, Inc.

Edited by I. Wilson

(Received 3 January 2006; received in revised form 3 May 2006; accepted 5 May 2006)
Available online 19 May 2006